Benchmarking two commonly used *Saccharomyces cerevisiae* strains for heterologous vanillin-β-glucoside production

Tomas Strucko, Olivera Magdenoska, Uffe H Mortensen *

Department of Systems Biology, Technical University of Denmark, 2800Kgs Lyngby, Denmark

ABSTRACT

The yeast *Saccharomyces cerevisiae* is a widely used eukaryotic model organism and a key cell factory for production of biofuels and wide range of chemicals. From the broad palette of available yeast strains, the most popular are those derived from laboratory strain S288c and the industrially relevant CEN.PK strain series. Importantly, in recent years these two strains have been subjected to comparative "-omics" analyzes pointing out significant genotypic and phenotypic differences. It is therefore possible that the two strains differ significantly with respect to their potential as cell factories for production of specific compounds. To examine this possibility, we have reconstructed a *de novo* vanillin-β-glucoside pathway in an identical manner in S288c and CEN.PK strains. Characterization of the two resulting strains in two standard conditions revealed that the S288c background strain produced up to 10-fold higher amounts of vanillin-β-glucoside compared to CEN.PK. This study demonstrates that yeast strain background may play a major role in the outcome of newly developed cell factories for production of a given product.

© 2015 The Authors. Published by Elsevier B.V. International Metabolic Engineering Society. This is an open access article under the CC BY-NC-ND license (http://creativecommons.org/licenses/by-nc-nd/4.0/).

1. Introduction

The recent achievements in the field of systems biology and metabolic engineering combined with a wide array of molecular biology tools has established the yeast *Saccharomyces cerevisiae* as a key cell factory for heterologous production of scientifically and industrially relevant products. The latter comprise a large variety of products ranging from low-value bulk chemicals and biofuels (e.g., ethanol) to food additives (e.g., flavors and colorants) and high value pharmaceuticals (e.g., recombinant proteins) (Kim et al., 2012; Hong and Nielsen, 2012). Today, a range of different *S. cerevisiae* strain backgrounds are available for the yeast community of which BY (S288c), W303 and CEN.PK are the most frequently used (van Dijken et al., 2000). The variety of strains has been developed by different laboratories to suit a range of diverse research goals within different disciplines such as genetics, physiology and biochemistry. For example, CEN.PK strain (Entian and Kötter, 2007), is a popular platform for physiological as well as metabolic engineering studies whereas S288c, the first eukaryote to be sequenced (Goffeau et al., 1996), was mainly used for genetic studies, but has in recent years been increasingly used as an alternative platform for metabolic engineering experiments (Kim et al., 2012; Hong and Nielsen, 2012). Specifically, recent surveys show that over the past ten years the two strains were used in more than 50% of the analyzes with CEN.PK series being the most popular (approx. 37%-CEN.PK *vs.* 24%-S288c and its derivatives) (Kim et al., 2012; Hong and Nielsen, 2012). The importance of the two strains as cell factories is further substantiated by an extensive multi-laboratory efforts which were made for systematic comparisons of S288c and CEN.PK (Rogowska-Wrzesinska et al., 2001; Canelas et al., 2010). Genetic differences of these strains were revealed first by microarray studies (Daran-Lapujade et al., 2003) and more recently genotype to phenotype relation was investigated after whole-genome sequencing of the CEN.PK113-7D strain (Otero et al., 2010; Nijkamp et al., 2012). For example, the sequencing comparison studies revealed that 83 genes were absent in CEN.PK relative to S288C (Nijkamp et al., 2012) and that more than 22,000 single nucleotide polymorphisms (SNPs) exist between the two strains. 13,000 of the SNPs are distributed in 1843 open reading frames (ORFs) and the activity of a large number of proteins may therefore differ in the two strains; especially since 35% of these SNPs result in amino-acid residue substitutions. The remaining 9000 SNPs, which are mainly distributed in the intergenic regions, may potentially impact gene expression and thereby protein levels in the two strains. The fact that the highest enrichment of SNPs was detected in genes involved in carboxylic acid, organic acid, and carbohydrate metabolism, as well as, in nitrogen, amino acid, lipid and aromatic compound metabolism suggests that the basic metabolism in the two strain background may be quite different (Otero et al., 2010). Importantly, based on the combined "-omics" analyzes, several phenotypic differences between the two strains were assigned to
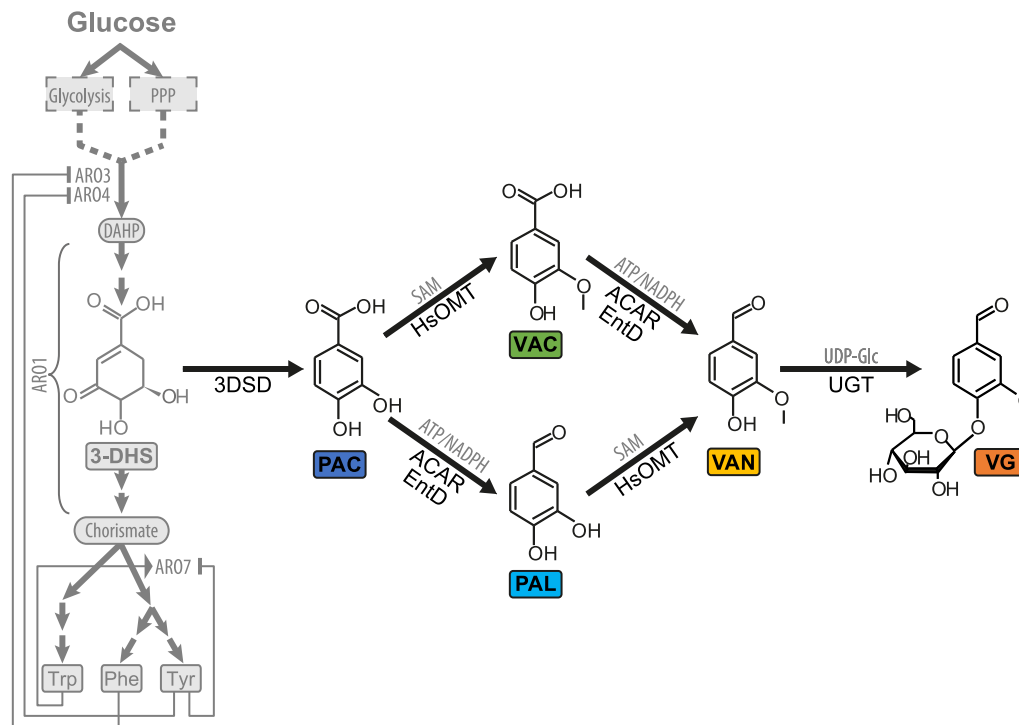
Fig. 1. *De novo* vanillin-β-glucoside pathway in *S. cerevisiae* assembled by Hansen et al. (2009). Colored boxes represent metabolites of the pathway: PAC – protocatechuic acid, PAL – protocatechuic aldehyde, VAC – vanillic acid, VAN – vanillin, VG – vanillin-glucoside. Black thick arrows show enzymatic reactions by heterologous enzymes: 3DSD – 3-dehydroshikimate dehydratase (*Podospora pauciseta*), ACAR – aromatic carboxylic acid reductase (*Neurospora sp.*), EntD – phosphopantetheine transferase (*Escherichia coli*), HsOMT – O-methyltransferase (*Homo sapiens*) and UGT – UDP-glycosyltransferase (*Arabidopsis thaliana*). Gray arrows and boxes (left side of the picture) represent simplified shikimate biosynthetic pathway and native parts of yeast metabolism: PPP – pentose phosphate pathway, DAHP – 3-deoxy-ᴅ-arabinoheptulosonate 7-phosphate, 3-DHS – 3-dehydroshikimic acid, Trp – tryptophan, Phe – phenylalanine, Tyr – tyrosine. Key enzymes of the shikimate pathway: ARO3 and ARO4 – DAHP synthase isoenzymes and ARO1 – pentafunctional enzyme catalyzing DAHP conversion to chorismate.

these mutations, e.g., differences in galactose uptake and ergosterol biosynthesis, etc. in two strains (Otero et al., 2010).

The fact that the two main *S. cerevisiae* backgrounds for construction of cell factories are genetically/phenotypically quite different raises the possibility that heterologous production of a given compound in CEN.PK and in S288c may result in significantly different yields. To examine this possibility, we therefore constructed comparable cell factories for vanillin-β-glucoside (VG) production in S288c and CEN.PK backgrounds. Importantly, all five relevant genes for VG production in *S. cerevisiae*, (see Fig. 1 and Hansen et al. (2009)) were integrated at phenotypically neutral and well defined locations in the yeast chromosome using a recently published integration platform (Mikkelsen et al., 2012). Moreover, in order for the engineered strains to be directly comparable, auxotrophies were eliminated by a sexual backcross to the corresponding wild-type strains. Remarkably, the physiological characterizations of both VG cell factories in two different cultivation modes revealed major differences in the VG production. Next, we examined the comprehensive "-omics" datasets for S288c and CEN.PK strains (Canelas et al., 2010) to look for plausible reasons for the different VG production profiles in the two genetic backgrounds. Together our analyzes serve as a step towards a scenario where the optimal genetic background for cell factory construction can be successfully selected based on a systems biology model for yeast cell factories.

2. Materials and methods

2.1. DNA cloning procedures

The DNA fragments used for vector construction were amplified by PCR with PfuX7 polymerase developed by Nørholm (2010) using the primers listed in the Table 1. Molecular coning was done by uracil-specific excision reagent (USER™) as previously described in (Geu-Flores et al., 2007; Nour-Eldin et al., 2006). Final constructs were validated by sequencing (StarSEQ® GmbH, Germany). The genes constituting the *de novo* VG pathway (1-*3DSD*, 2-*ACAR*, 3-*EntD*, 4-*HsOMT*, and 5-*UGT*) and a set of bidirectional promoter (pPGK1/pTEF1) were amplified by PCR from the appropriate vector templates (see Table 2). The pathway genes and promoters were assembled into vectors designed to integrate on chromosome XII (Mikkelsen et al., 2012). A total of three plasmids were produced: pXII1-23 (pPGK1::ACAR; pTEF1::EntD), pXII2-54 (pPGK1::UGT; pTEF1::HsOMT) and pXII5-01 (pTEF1::3DSD), see Fig. S1. For a full list of plasmids used or constructed in this work see Table 2.

2.2. Strain construction

The genotype and source of the strains used in this study is given in the Table 3. Two different background strains CEN.PK113-11C and X2180-1A (isogenic to S288c (Mortimer and Johnston, 1986)) were used as hosts for reconstruction of the de novo vanillin-β-glucoside (VG) pathway. All yeast constructs were generated by high efficiency transformation method (lithium acetate/polyethylene glycol/single carrier DNA) previously described by Gietz et al. (1992).

To construct two yeast strains containing the VG pathway, vectors pXII1-23, pXII2-54 and pXII5-01 harboring the following genes (*ACAR* and *EntD*), (*UGT* and *HsOMT*) and (*3DSD*), respectively, were digested with *Not*I restriction enzyme (Fermentas-Thermo Fisher Scientific) and gel-purified using illustra GFX PCR DNA and Gel Band Purification Kit (GE Lifesciences). The individual gene

Table 1
List of the primers used in this study. All sequences are presented in 5′–3′ direction, standard capital letter are gene specific sequences, **bold** letters represent USER specific tails, regular underline letters represent targeting sequences for appropriate gene deletions. *Italic* letters represent translational enhancer sequence (Nakagawa et al., 2008; Cavener and Ray, 1991).

Name	Sequence
Primers for cloning purposes	
PGK_R-	**ACCCGTTGAU**GCCGCTTGTTTTATATTTGTTG
TEF_F+	**CGTGCCGAU**GCCGCACACACCATAGCTTC
TEF_R+	**ACGTATCGCU**GTGAGTCGTATTACGGATCCTTG
DSD_F+	**AGCGATACGU***AAAAA*ATGCCTTCCAAACTCGCC
DSD_R+	**CACGCGAU**TTACAAAGCCGCTGACAGC
ACAR_F-	**ATCAACGGGU***AAAAA*ATGGCTGTTGATTCACCAGATG
ACAR_R-	**CGTGCCGAU**CTTATAACAATTGTAACAATTCCAAATC
hOMT_F+	**AGCGATACGU***AAAAA*ATGGGTGACACTAAGGAGCAA
hOMT_R+	**CACGCGAU**CTTATGGACCAGCTTCAGAACC
PPT1_F+	**AGCGATACGU***AAAAA*ATGGTCGATATGAAAACTACGC
PPT1_R+	**CACGCGAU**TTAATCGTGTTGGCACAGC
UGT1_F-	**ATCAACGGGU***AAAAA*ATGCATATCACAAAACCACACG
UGT1_R-	**CGTGCCGAU**ACTAGGCACCACGTGACAAGTC
Deletion primers	
BGL1_del_F	ATTTTTTGTTTACTTTCTTTTTCTAGTTAATTACCAACTAAACTTCGTACGCTGCAGGTC
BGL1_del_R	CATTAGAAAATTCAGCTAAAATGAGCGGACTGAGGGCGACTAGTGGATCTGATATCACCTA
ADH6_del_F	GAGGAAGAAATTCAACACAACAACAAGAAAAGCCAAAATCCTTCGTACGCTGCAGGTC
ADH6_del_R	GTTAAAAAGAAAGGAGCTACATTTATCAAGAGCTTGACAACTAGTGGATCTGATATCACCTA
Verification primers	
XII-1-up-out-sq	CTGGCAAGAGAACCACCAAT
XII-2-up-out-sq	CGAAGAAGGCCTGCAATTC
XII-5-up-out-sq	CCACCGAAGTTGATTTGCTT
C1_TADH1_F	CTTGAGTAACTCTTTCCTGTAGGTC
BGL1_VF	TCATCCTCCCTGTGTTTACA
BGL1_VR	AGTTGAAACAGAGGATAAGGTG
ADH6_VF	GTTTTGCTTTTTTCTCTGGG
ADH6_VR	GGAGTATCAACCACTAAAGCG
Primers for sequencing	
S1_TEF_F	CGGTCTTCAATTTCTCAAGTTTC
S1_PGK_F	CAAGGGGGTGGTTTAGTTTAGT
S1_ACAR_F	CATTGTTCGTTCCAGACACTGAC
S2_ACAR_F	GAAATTGTCTCAAGGTGAGTTCG
S3_ACAR_F	TTTGGGTAGATTCTTGTGTTTGG
YF19	AAAAAATAAATAGGGACCTAGACTTCA
YF21	GACCTACAGGAAAGAGTTACTCAAGAAT

Table 2
List of the plasmids used and constructed in this study.

Name	Genetic element	Reference
pXII1–23	*pPGK1::ACAR, pTEF1::EntD*	This study
pXII2–54	*pPGK1::UGT, pTEF1::HsOMT*	This study
pXII5–01	*pTEF1::3DSD*	This study
pXII1	–	Mikkelsen et al. (2012)
pXII2	–	Mikkelsen et al. (2012)
pXII5	–	Mikkelsen et al. (2012)
pSP–G2	*pPGK1;pTEF1*	Partow et al. (2010)
pJH500	*3DSD*	Hansen et al. (2009)
pJH674	*ACAR*	Hansen et al. (2009)
pJH589	*EntD*	Hansen et al. (2009)
pJH543	*HsOMT*	Hansen et al. (2009)
pJH665	*UGT*	Hansen et al. (2009)
pUG6	*KanMX*	Güldener et al. (1996)
pSH47	*Cre recombinase*	Güldener et al. (1996)

targeting substrates were transformed iteratively into both yeast strain backgrounds in three consecutive transformations. To prevent undesired production of toxic intermediates especially protocatechuic aldehyde (PAL), the *3DSD* gene was cloned at the latest step. After each round of transformation the URA3 marker was eliminated by direct repeat recombination and counter-selection on 5-FOA (Boeke et al., 1984) allowing the URA3 marker to be recycled.

Complete gene deletions of *BGL1* and *ADH6* were achieved using method described by Güldener et al. (1996). PCR fragment

carrying *loxP*-KanMX-*loxP* flanked by 40nt long segment homologous to sequences of Up- and Down-stream of the appropriate open reading frame (ORF) to be deleted were amplified form plasmid pUG6. The KanMX marker was excised by expressing Cre recombinase from the vector pSH47 (Güldener et al., 1996). All gene targeting events were validated by diagnostic PCR using specially designed primer pairs (see Table 1).

To eliminate any auxotrophies, two engineered strains S-VG-aux and C-VG-aux were sexually crossed to S288c and CEN.PK110-16D, respectively. This resulted in two final prototrophic vanillin-β-glucoside producing yeast strains S-VG (S288c based) and C-VG (CEN.PK based). Genetic cross and selection procedures were performed as described in (Treco and Winston, 2008). Schematic flowchart representing the strain construction is depicted in Fig. S2.

2.3. Media

For cloning purposes lysogeny broth (LB) (Bertani, 1951) supplemented with 100 mg/L of ampicillin (Sigma-Aldrich) was used for growing of *Escherichia coli* DH5α.

All media used for genetic manipulations of yeast were prepared as previously described by Sherman et al. (1986), with minor modifications of synthetic medium where leucine concentration was doubled to 60 mg/L. All yeast transformants with gene integrations were selected on synthetic complete media missing uracil (SC-ura). For subsequent round of transformations

Table 3
List of the yeast strains used in this study.

Name	Genotype	Reference
X2180-1A (ura3)	*MATa SUC2 mal mel gal2 CUP1 ura3-52*	Public domain (Mortimer and Johnston, 1986)
S288c	*MATα SUC2 gal2 mal mel flo1 flo8-1 hap1 ho bio1 bio6*	ATCC 204508
CEN.PK113-11C	*MATa MAL2-8C SUC2 ura3-52 his3Δ*	Peter Kötter[a]
CEN.PK110-16D	*MATα MAL2-8C SUC2 trp1-289*	Peter Kötter[a]
C-VG-aux	*MATa MAL2-8C SUC2 ura3-52 his3Δ XII2(pTEF1-HsOMT, pPGK1-UGT) XII1(pTEF1-PPT, pPGK1-ACAR) XII5 (pTEF1-3DSD) Δbgl1::loxP Δadh6::KanMX*	This study
S-VG-aux	*MATa SUC2 gal2 mal mel ura3-52 XII2(pTEF1-HsOMT, pPGK1-UGT) XII1(pTEF1-PPT, pPGK1-ACAR) XII5 (pTEF1-3DSD) Δbgl1::loxP Δadh6::KanMX*	This study
C-VG	*MATα MAL2-8C SUC2 XII2(pTEF1-HsOMT, pPGK1-UGT) XII1(pTEF1-PPT, pPGK1-ACAR) XII5(pTEF1-3DSD) Δbgl1::loxP Δadh6::KanMX*	This study
S-VG	*MATα SUC2 gal2 mal mel XII2(pTEF1-HsOMT, pPGK1-UGT) XII1(pTEF1-PPT, pPGK1-ACAR) XII5(pTEF1-3DSD) Δbgl1::loxP Δadh6::KanMX*	This study

[a] Institut für Mikrobiologie, der Johan Wolfgang Goethe-Universität, Frankfurt am Main, Germany.

URA3 marker was recycled through direct repeat recombination and selected on synthetic complete media containing 30 mg/L uracil and 740 mg/L 5-fluoroorotic acid (5-FOA) (Sigma-Aldrich).

Yeast transformants with necessary gene deletions were selected on Yeast Extract Peptone Dextrose (YPD) plates supplemented with 200 mg/L of G418 (Sigma-Aldrich) (Güldener et al., 1996). The medium composition is as follows: 10 g/L of yeast extract, 20 g/L of peptone and 20 g/L of glucose and 20 g/L of agar.

A defined minimal medium previously described by Verduyn et al. (1992) with glucose as a carbon source was used for *S. cerevisiae* cultivations in batch and chemostat cultures. For batch cultivations the medium was supplemented with 30 g/L of glucose (Canelas et al., 2010), whereas for feed media for continuous cultivations contained 7.5 g/L of glucose. The medium was composed of: 7.5 g/L $(NH_4)_2SO_4$, 3 g/L KH_2PO_4, 0.75 g/L Mg_2SO_4, 1.5 mL/L trace metal solution, 1.5 mL/L vitamins solution, 0.05 mL/L antifoam 204 (Sigma-Aldrich). Trace metal solution contains 3 g/L $FeSO_4 \cdot 7H_2O$, 4.5 g/L $ZnSO_4 \cdot 7H_2O$, 4.5 g/L $CaCl_2 \cdot 6H_2O$, 0.84 g/L $MnCl_2 \cdot 2H2O$, 0.3 g/L $CoCl_2 \cdot 6H_2O$, 0.3 g/L $CuSO_4 \cdot 5H_2O$, 0.4 g/L $NaMoO_4 \cdot 2H_2O$, 1 g/L H_3BO_3, 0.1 g/L KI and 15 g/L $Na_2EDTA \cdot 2H_2O$. Vitamins solution includes 50 mg/L D-biotin, 200 mg/L para-amino benzoic acid, 1.0 g/L nicotinic acid, 1.0 g/L Ca-pantothenate, 1.0 g/L pyridoxine HCL, 1.0 g/L thiamine HCl and 25 mg/L minositol. Glucose was autoclaved separately and vitamins solutions were sterile filtered (pore size 0.2 μm Ministart®-Plus, Sartorius AG, Germany) and added after autoclavation.

2.4. Batch and chemostat cultivations

For each biological replica separate colonies of engineered yeast strains from YPD plate were inoculated to the 0.5 L shake flasks with 50 mL of the previously described minimal medium (pH 6.5). Pre-cultures were incubated in an orbital shaker set to 150 rpm at 30 °C until mid-exponential phase $OD_{600} \approx 5$ and directly used for inoculation. In this experiment, batch cultivations were performed in duplicates and continuous cultures – in triplicates.

Batch cultivations were performed under aerobic conditions in 1 L fermenters equipped with continuous data acquisition (Sartorius, B. Braun Biotech International, GmbH, Melsungen, Germany) with a working volume of 1 L. Fermenters were inoculated with initial $O.D._{600}=0.05$. To ensure aeration a stirrer speed was set to 600 rpm and airflow rate to 1.0 v.v.m. (60 L/h). The temperature was maintained at 30 °C during the cultivation and $pH=5.0$ level was controlled by automatic addition of 2 M NaOH or 2 M H_2SO_4. The batch cultures were sampled in regular intervals through both glucose and ethanol growth phases. Glucose-limited chemostat cultures were grown in the same conditions as

previously described for batch cultivations. Chemostats were initiated as batch cultivations with starting glucose concentration of 15 g/L and $OD_{600}=0.05$ and switched to continuous mode in early exponential phase. Minimal medium was fed at a constant dilution rate of 0.1 h^{-1} (Canelas et al., 2010). The working volume of 1 L was kept constant by a level based outlet. Samples were taken after at least five residence times (50 h) of constant biomass and carbon dioxide concentration readings.

In both cultivation experiments exhaust gas composition was constantly monitored by off gas analyzer (1311 Fast response triple gas, Innova) combined with Mass Spectrometer (Prima Pro Process MS, Thermo Fisher Scientific, Winsford UK). No elevated ethanol concentration in the exhaust was detected.

The biomass concentration was monitored by measuring both optical density at 600 nm wavelength (OD_{600}) and cell dry weight (DW) in the cultivation broth. OD_{600} was estimated using a UV mini 1240 spectrophotometer (Shimadzu, Kyoto, Japan), biomass samples were diluted with distilled water to achieve OD_{600} reading within 0.1–0.4 range. DW measurements were performed using polyethersulfone (PES) filters with a pore size of 0.45 μm Montamil® (Membrane Solutions, LLC). The filters were pre-dried in a microwave oven at 150 W and weighed. A known volume of cultivation broth (5 mL) was filtered and then washed with approx. 15 mL of distilled water. Finally, the filters with biomass were dried in the microwave oven at 150 W and cell DW was determined (Olsson and Nielsen, 1997).

2.5. Extracellular metabolite measurements

Extracellular metabolites were determined by high performance liquid chromatography (HPLC) analysis. Two distinct HPLC methods were applied for analysis of different groups of extracellular metabolites.

The submerged cultivation samples for yeast primary metabolites were centrifuged at 12,000g for 2 min, supernatant was transferred to a new tube and stored at −20 °C until further analysis. Glucose, ethanol, glycerol, pyruvate, succinate and acetate were determined by high performance liquid chromatography (HPLC) analysis using an Aminex HPX-87H ion-exclusion column (Bio-Rad Laboratories, Hercules, CA). The column temperature was kept at 60 °C and the elution was performed using 5 mM H_2SO_4 with constant flow rate of 0.6 mL min^{-1}. Metabolite detection was performed by a RI-101 differential refractometer detector (Shodex) and an UVD340U absorbance detector (Dionex) set at 210 nm.

Samples for quantification of vanillin-β-glucoside and its pathway metabolites were prepared as follows: 1 mL of cultivation broth and 1 mL of 96% EtOH was carefully mixed by vortex and centrifuged at 12,000g for 2 min, supernatant was transferred to a

new tube and stored at -20 °C until further analysis. Extracellular vanillin-β-glucoside (VG), vanillin (VAN), protocatechuic acid (PAC), protocatechuic aldehyde (PAL) and vanillic acid (VAC) were quantified using Agilent 1100 series equipment with a Synergi Polar-RP 150×2 mm $4\,\mu$ column (Phenomenex). A gradient of acetonitrile (ACN) with 1% tetra-fluoroacetic acid (TFA) and water with 1% TFA at a constant flow rate of 0.5 mL/min was used as mobile phase. The elution profile was as follows: 5% ACN – 1 min, 5% ACN to 30% ACN – 8 min, 30% ACN to 100% ACN – 1 min, 100% ACN − 1 min, 100% ACN to 5% ACN – 3 min. The column was kept at 40 °C and metabolite detection was performed using a UV diode-array detector set to 230 and 280 nm.

2.6. Intracellular metabolite measurements

Samples for intracellular co-factor metabolites were taken during steady state conditions at the end of continuous cultivation. The samples were quenched and extracted as previously described by Villas-Bôas et al. (2005); 5 mL of culture broth was sprayed into pre-cooled (-40 °C) falcon tube containing 20 mL of 60% methanol, spun down for 2 min at $5000g$ in precooled centrifuge (-10 °C) and extracted using boiling ethanol method (Villas-Bôas et al., 2005) followed by evaporation under nitrogen. The samples were re-dissolved in $300\,\mu$L eluent A (10 mM tributylamine and 10 mM acetic acid). The analysis was carried out on an Agilent 1290 binary UHPLC system coupled with an Agilent 6460 triple quadrupole mass spectrometer (Torrance, CA, USA). The MS was operated in negative ion and multiple reactions monitoring mode. Separation of $0.5\,\mu$L samples was performed by ion-pair chromatography, as described in detail in Magdenoska et al. (2013) using 10 mM tributylamine as ion pair reagent. The gradient used was: 0–12 min 0–50% B, 12–12.5 min 50–100% B, 12.5–14 min 100% B, 14–14.5 min 100–0% B, 14.5–19.5 min 0% B. External standard calibration method was used for quantification. The calibration curves were constructed by preparing calibration solutions ranging from 1 to 100 μg/mL for ATP and 0.3–25 μg/mL for NADPH and UDP-glucose. Both the quenched extracts and the calibration solutions were spiked with 60 μL mixture containing 150 μg/mL [U − ^{13}C] ATP. The quantification was carried out using Mass Hunter Quantitative analysis software (version B.06.00).

3. Results

3.1. De novo pathway reconstruction in CEN.PK and S288c backgrounds

To compare CEN.PK and S288c for their ability to produce VG in a fair manner, it was necessary to insert all genes identically in both strain backgrounds. In the original VG producing strain, the individual genes of the pathway were inserted by repeated integrations into the *TPI1* promoter region in an S288c based strain (Hansen et al., 2009). Consequently, the gene order is ill-defined and not easy to reconstruct in CEN.PK. We therefore introduced the VG pathway in the two strain backgrounds, S288c (isogenic isolate X2180-1A (Mortimer and Johnston, 1986)) and CEN.PK113-11C (Entian and Kötter, 2007) in a defined manner. Specifically, the five genes used by Hansen et al. (2009) for VG production were integrated into three sites located on chromosome XII (see Fig. 2), which are part of a defined gene expression platform we have previously established (Mikkelsen et al., 2012). Importantly, prior to integration, we compared the up- and downstream sequences at these integration sites in CEN.PK and S288c and found that they differ by only a single SNP, a C in CEN.PK and G in S288c, which is present in the upstream targeting sequence of the XII-5 site. The five genes are therefore inserted into a genetic context, which is
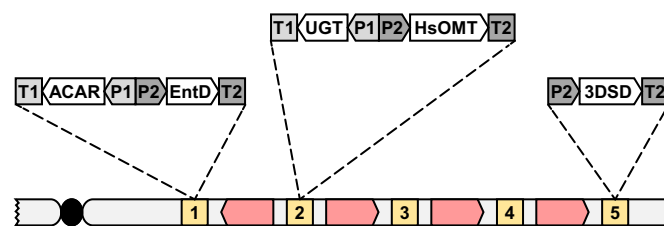
Fig. 2. Schematic representation of VG pathway reconstruction in two different *S. cerevisiae* background strains. T1, T2 – terminators of *ADH1* and *CYC1*, respectively; P1, P2 – promoters of *PGK1* and *TEF1*, respectively. Red arrows represent essential genetic elements of *S. cerevisiae* and numbered yellow boxes are integration sites characterized by Mikkelsen et al. (2012). (For interpretation of the references to color in this figure legend, the reader is referred to the web version of this article.)

essentially identical. Additionally, two genes *ADH6* and *BGL1* were deleted in both strains to minimize unwanted side reactions with VG pathway metabolites. Finally, for both genetic backgrounds, auxotrophic markers were eliminated by sexual back crossing to wild-type variants of the two strain backgrounds to produce two prototrophic VG producing strains, C-VG (CEN.PK based) and S-VG (S288c based), which we used for further analysis.

3.2. Physiological characterization of vanillin-β-glucoside producing strains during batch and continuous fermentations

Before evaluating the VG production ability of the two strain backgrounds, we first assessed whether VG production affected the overall physiology of the C-VG and S-VG strains. Hence, they were grown in batch and as continuous cultures in well-controlled bioreactors under standard laboratory cultivation conditions (Canelas et al., 2010). Like for wild-type strains, the overall growth profiles exhibited by the S-VG and C-VG strains in batch reactors were composed by two growth phases. One initial growth phase where all glucose was fermented (GF – phase); followed, after the diauxic shift, by a second growth phase where all accumulated ethanol was respiro-fermented (ER – phase), see Fig. 3. We note that the specific biomass yield on glucose (Table 4) appeared higher (14%) in C-VG as compared to S-VG, but in our experiment this difference was not significant ($p > 0.33$). A similar difference has previously been observed for the parental S288c and CEN.PK strains grown at the same conditions (van Dijken et al., 2000; Canelas et al., 2010). It has previously been shown that CEN.PK grows faster than S288c at these conditions, $\mu_{max} \approx 0.4\ \text{h}^{-1}$ vs. $\mu_{max} \approx 0.3\ \text{h}^{-1}$, respectively (Canelas et al., 2010; Otero et al., 2010). In contrast, C-VG and S-VG grew slower than the corresponding wild-type strains and both strains displayed identical growth rates on glucose ($\mu_{max} \approx 0.2\ \text{h}^{-1}$). Further analysis of the cultivation broth obtained at different time points during growth, showed that the production profiles of five primary metabolites (ethanol, pyruvate, succinate, glycerol, and acetate) in the central carbon metabolism of S-VG and C-VG were similar to what has previously been observed with the corresponding wild-type strains (Fig S3). Among the remaining parameters – r_{Glc}, r_{Eth}, and r_{Gly}, only the latter varied between the two strains as it was approx. three-fold higher in the S-VG ($p < 0.002$). Finally, we also note that S-VG displayed a growth deficiency during the ER phase which was nearly twice as long with S-VG (23 h) than with C-VG (12 h) partly due to a much longer delay from the diauxic shift to exponential growth is resumed. This deficiency has also been previously reported for wild-type S288c (Otero et al., 2010).

In chemostats, steady-state conditions with constant production of biomass as well as stable readings of carbon dioxide and oxygen by the off-gas analyzer where obtained for both strain
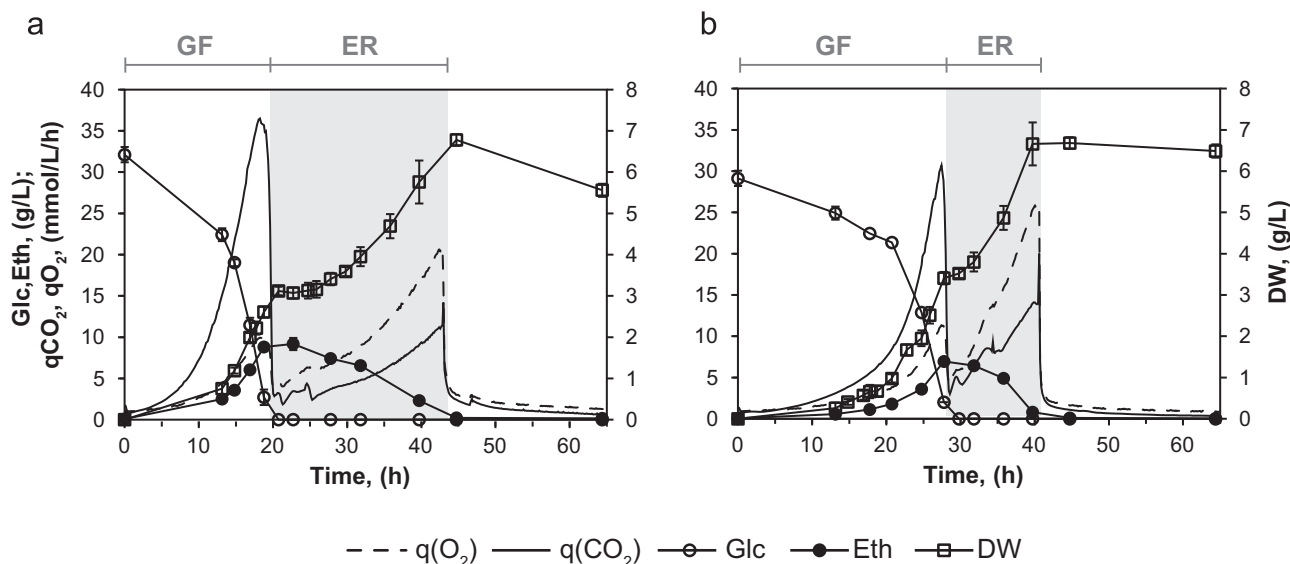
Fig. 3. Growth profiles of the two strains in the batch cultures: (a) S-VG and (b) C-VG. Gray areas represent ethanol respiration (ER) phase; GF – glucose fermentation. qCO_2 – carbon dioxide production rate, qO_2 – oxygen consumption rate; Glc – glucose, Eth – ethanol and DW – cell dry weight. Error bars represent standard deviation, $n=2$.

Table 4

Physiologic parameters of the two engineered strains. Y_{sx} – biomass yield on glucose, r – specific metabolite production or consumption rates (C-mmol/g(DW) h); Glc –glucose, Eth – ethanol and Gly – glycerol. NA – not applicable and ND – not detected. The yield coefficient Y_{sx} for biomass is calculated based on a molecular weight for biomass of 26.4 g/C-mol (Lange and Heijnen, 2001). Errors represent standard deviation, $2 \le n \le 3$.

Cultivation mode	Batch		Chemostat	
Strain	S-VG	C-VG	S-VG	C-VG
Glucose μ, h^{-1}	0.209 ± 0.002	0.199 ± 0.002	$(0.1)^*$	$(0.1)^*$
Ethanol μ, h^{-1}	0.05 ± 0.01	0.08 ± 0.01	NA	NA
Y_{sx} (C-mol/C-mol)	0.133 ± 0.014	0.151 ± 0.001	0.56 ± 0.02	0.60 ± 0.02
$-r_{Glc}$	60.7 ± 8.0	49.9 ± 0.60	6.81 ± 0.29	6.37 ± 0.20
r_{Eth}	25.9 ± 3.1	20.9 ± 3.00	ND	ND
r_{Gly}	4.05 ± 0.05	1.40 ± 0.13	ND	ND

    * The dilution rate used in this study.

Fig. 4. Final yields (45 h after inoculation) of VG, its intermediates, and TCV produced by S-VG (blue) and C-VG (yellow) during batch cultivation. Error bars represent standard deviation, $n=2$. (For interpretation of the references to color in this figure legend, the reader is referred to the web version of this article.)

backgrounds. For the C-VG strain this was achieved in less than 5 residence times (50 h) after feeding was initiated, whereas for the S-VG strain it took more than 8 residence times (80 h), see Fig S4. Importantly, at a dilution rate of 0.1 h^{-1}, both strains propagated exclusively by glucose respiratory metabolism (Van Hoek, 1998) as no production of ethanol, glycerol and organic acids was observed (see Table 4). The C-VG strain produced significantly more (seven percent, $p < 0.01$) biomass as compared to S-VG, on the contrary, the specific glucose uptake rate was approx. seven % higher ($p < 0.01$) in S-VG strain.

3.3. High VG yields with S288c are generated during its prolonged ethanol respiratory growth phase

VG production in the S-VG and C-VG strains was initially compared at 45 h after both cultures have reached stationary phase. In the original VG producing strain constructed by Hansen et al. (2009), various levels of intermediates were observed due to an unbalanced heterologous VG pathway (Hansen et al., 2009), (Brochado et al., 2010). In agreement with this, analyzes of the extracellular metabolite levels in the cultivation broth showed that PAC, PAL, VAC, and VAN accumulated in both S-VG and C-VG in batch cultivation. The yields of each of the intermediates were
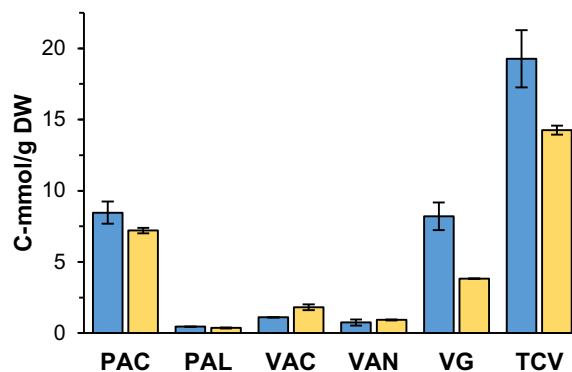
similar in the two strains (Fig. 4) with PAC being by far the most prominent metabolite. In fact, PAC accounted for ~70- and 75% of the carbon ending up as intermediates in C-VG and S-VG strains, respectively. However, when the two strains were analyzed for VG production, we surprisingly observed that twice as much VG was produced with the S-VG strain than with the C-VG strain ($p < 0.05$). This finding prompted us to determine and compare the production of VG and its intermediates of the two strains during the different growth phases throughout the entire batch cultivation (Fig. 5A and B). The VG yields were almost identical with the two strains during the GF phase (Fig. 5C). The total carbon ending up in VG pathway metabolites (TCV) is 14% lower in C-VG as compared to S-VG. This effect is mainly due to less accumulated PAC in C-VG (37% less in C-VG, $p < 0.05$). In contrast, with S-VG, a two-fold higher ($p < 0.05$) VG yield was generated during the ER phase than with C-VG despite that the amounts of intermediates accumulating at the end of the phase were similar in both strains (see Fig. 5C). As a result, TCV was 45% higher with S-VG as compared to C-VG. Yields and productivities on glucose during exponential growth and during steady state condition are represented in the Table S1).

To further understand why VG yields were higher with S-VG than with C-VG, we determined whether production of VG and
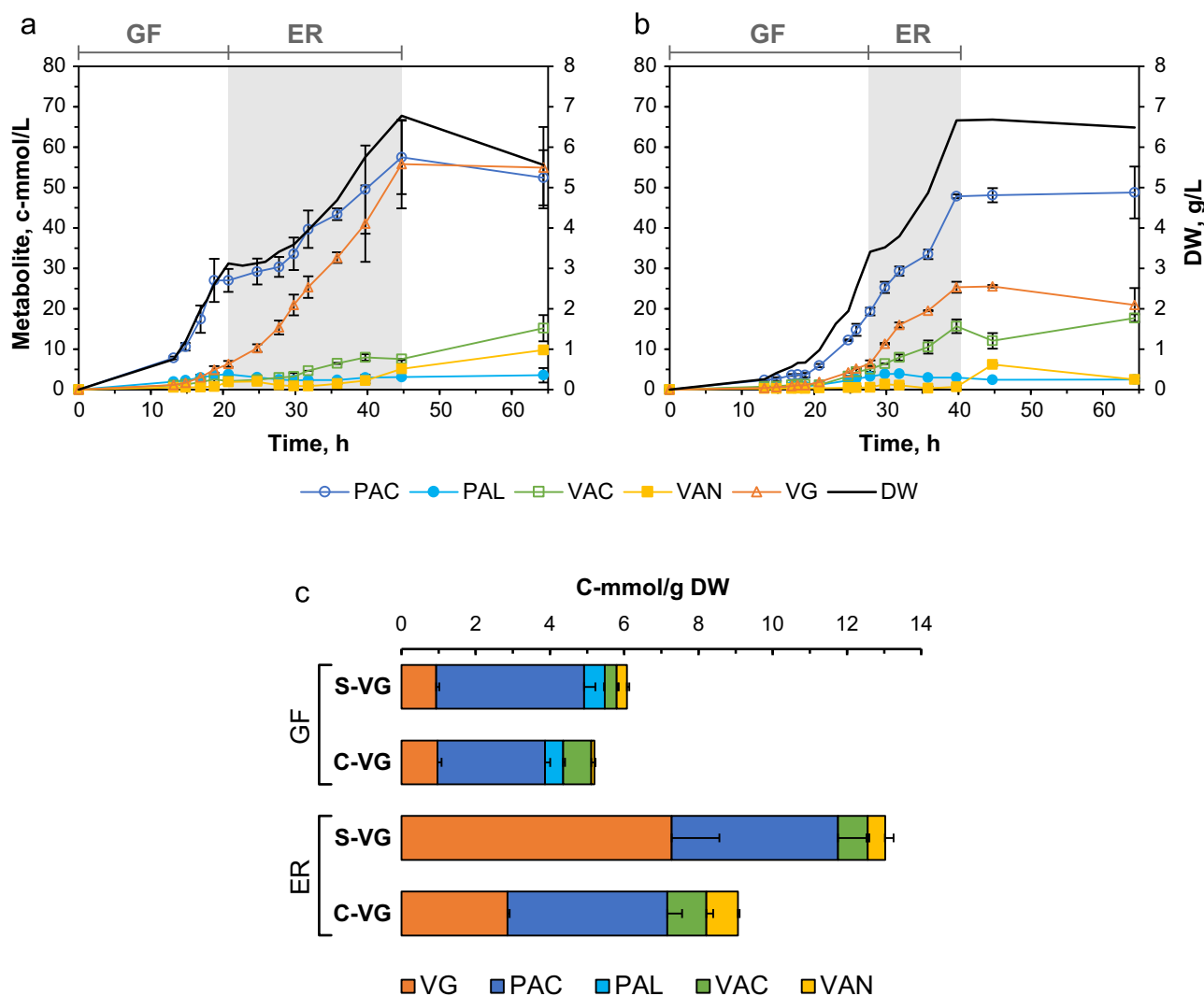
Fig. 5. Metabolic profiles of VG and its intermediates in batch cultivation in (a) S-VG and (b) C-VG strains. (c) Accumulation of VG pathway metabolites during the glucose fermentation (GF) and ethanol respiration (ER) growth phases.

VG-intermediates was proportional to biomass during all time-points. Based on this analysis, we observed for both strains that the efficiencies of TCV, VAC and VG production were higher in the ER phase as compared to the GF phase. In contrast, for both strains PAC was produced with equal efficiency in the two phases Fig. 6. After the diauxic shift, C-VG quickly entered a new state where these metabolites were produced in amounts proportional to biomass. With S-VG such states are also achieved for TCV, PAC and VAC although, for TCV and VAC, more time was required for these states to be reached in this strain as compared to C-VG. In contrast, with S-VG a state where VG was produced proportionally to bio-mass was never achieved as the VG production efficiency increased during the entire phase, see Fig. 6D.

3.4. Steady-state VG production at glucose limitation is higher in S288c than in CEN.PK

Next, we investigate VG production in continuous cultures where we could obtain strictly glucose respiratory conditions for both strains, see above. Dramatically, this analysis revealed that the amounts of TCV and VG were significantly increased to levels four- and ten-fold higher with S-VG than with the C-VG strain ($p < 9E-9$, $p < 2E-10$, respectively), see Fig. 7. When the levels of intermediates were inspected, we observed that with S-VG, the majority (68%) of the TCV ended up in VG, whereas the rest of the carbon ended up in PAC (18%) and in VAC (13%). In contrast, VG constituted only 20% of the TCV in the C-VG strain. The remaining carbon was mainly ending up in VAC (approx. 70%) and only little (less than 5%) in PAC.

Four co-factors, ATP, NADPH, SAM and UDP-Glc, are used for formation of VG. In the paper by Canelas et al. (2010) where "-omics" data for the two background strains were compared, the levels of three of these cofactors (ATP, NADPH and UDP-Glc) were measured. We were able to quantify ATP and therefore determined the concentrations of this metabolite in C-VG and S-VG to investigate whether ATP levels were altered due to the presence of the VG pathway. Analysis of samples obtained at steady state showed that concentrations of ATP were 10.6 μmol/g DW and 8.5 μmol/g DW for C-VG and S-VG, respectively. These numbers are somewhat higher than the corresponding numbers reported by Canelas et al. and this may be due to lab to lab differences. Importantly, the relative ATP levels of the two strains (C-VG to S-VG) is 1.2 in our experiment as well as in theirs (Canelas et al., 2010). This indicates that the presence of the VG pathway does not change ATP levels in the two strains despite that 10-fold more VG is formed in S-VG as compared in to C-VG. Due to the absence of internal standards for NADPH and UDP-Glc, we were not able to compare our data with those in the literature. However, UDP-Glc
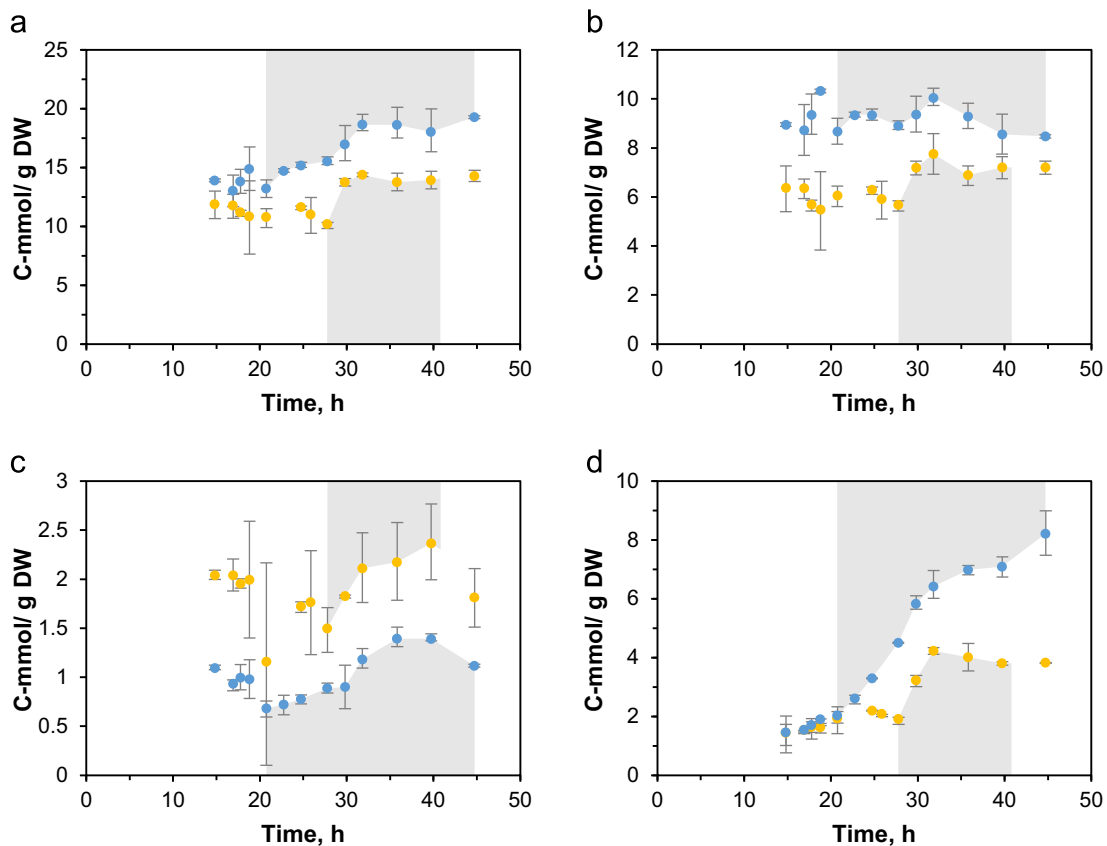
Fig. 6. Distribution of VG pathway metabolite per biomass throughout entire batch cultivation: (a) TCV, (b) PAC, (c) VAC, (d) VG. Blue circles data for S-VG, yellow circles – C-VG. Gray areas represent ethanol respiration phase (narrow in C-VG and wide in S-VG). Error bars represent standard deviation, $n=2$. The amounts of PAL and VAN constituted less than seven percent of TCV at all time points and were not depicted. (For interpretation of the references to color in this figure legend, the reader is referred to the web version of this article.)
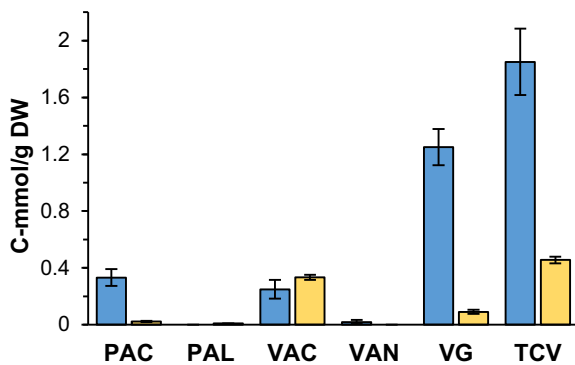

Fig. 7. Yields of VG, its intermediates, and TCV produced by S-VG (blue) and C-VG (yellow) during continuous cultivation; (a) Average of last three samples with more than one retention time in between. Error bars represent standard deviation, $n=3$. (For interpretation of the references to color in this figure legend, the reader is referred to the web version of this article.)

levels were 0.5 μmol/g DW for both strains. These results were also confirmed by a high resolution mass spectrometer, where similar chemical profiles were obtained for both strains. The NADPH levels measured in C-VG and S-VG in our study were close to the limit of detection preventing a comparison between the two strains.

4. Discussion

The importance of *Saccharomyces cerevisiae* in the development of novel cell factories is demonstrated by the large number of industrially relevant substances that can now be produced in this organism (Kim et al., 2012; Hong and Nielsen, 2012; Nevoigt, 2008). Several laboratory yeast strains have been used for this purpose with S288c and CEN.PK being the most popular (Hong and Nielsen, 2012; Canelas et al., 2010). However, despite that the two strains are genetically and physiologically very different (van Dijken et al., 2000; Canelas et al., 2010; Otero et al., 2010; Nijkamp et al., 2012); these differences are rarely used to determine, which strain background should be chosen as a cell factory for *de novo* production of a given compound. In this study, we therefore investigated whether choice of yeast strain background for production of vanillin-β-glucoside (VG) is an issue that can be advantageously considered. Our finding that heterologous production of VG was dramatically more efficient in an S288c based strain compared to CEN.PK in both batch and continuous cultivations demonstrates that this is indeed the case.

Our physiological characterizations of the C-VG and S-VG strains show that the S-VG strain produces significantly more VG in both batch and continuous cultivations. One explanation could be a higher flux of carbon into the VG pathway in the S-VG strain. In agreement with this, both the first intermediate in the VG pathway (PAC) and TCV accumulate to significant higher levels with S-VG as compared to with C-VG during both continuous and batch cultivations, see Figs. 4 and 7. For batch cultivation, we note this is true at all time points examined, see Fig. 6.

Carbon for VG production is recruited from the shikimate pathway, which is a part of the aromatic amino acid biosynthesis and, which is well characterized in yeast (Teshiba et al., 1986; Braus, 1991). The pathway is tightly regulated via two 3-deoxy-D-arabinoheptulosonate 7-phosphate (DAHP) synthase isoenzymes Aro3 and Aro4, which are feedback inhibited by phenylalanine and

tyrosine, respectively (Fig. 1). In this context, we note that in the case of CEN.PK derived strains, the flux through the shikimate pathway is increased more than four-fold if feedback inhibition is eliminated (Luttik et al., 2008); and that this feature has been successfully exploited in a metabolic strategy to increase the yield of CEN.PK strains producing the plant flavonoid naringenin, which is derived from phenylalanine and tyrosine (Koopman et al., 2012). Interestingly, two of the genes in the shikimate pathway, *ARO1* and *ARO3*, contain ten SNPs that result in amino acid substitutions. Moreover, a large number of SNPs are distributed in the up- and downstream regions of the genes in the shikimate pathways. It is therefore likely that the level and/or activities of enzymes of the shikimate pathway are different in the two strain backgrounds. In agreement with this, the available "-omics" datasets presented by Canelas et al. (2010) show that the intracellular concentration of shikimic acid (the direct metabolite of 3-DHS) is significantly higher in S288c than in CEN.PK strains at similar conditions in batch and continuous cultivations. Moreover, they also reported that under chemostat conditions CEN.PK strains are able to maintain higher intracellular amino-acid pools, which was suggested, and later shown, to be a result of increased protein turnover rate (Hong et al., 2012).

In VG producing strains, we therefore speculate that higher concentrations of intracellular aromatic amino acids in C-VG might inhibit Aro3 and Aro4 leading to a decreased flux towards 3-DHS and consequently to a lower capacity for VG production. When the genomes of S288c and CEN.PK SNPs were compared, several SNPs exist in genes encoding for enzymes involved in the amino acid and aromatic compound metabolism. For example, we have compared ORFs sequences of several *ARO* genes in the strains, see Table 5. Importantly, the gene of the pentafunctional enzyme Aro1 (which is directly involved in synthesis of 3-DHS) contains 15 SNPs, of which, seven results in non-synonymous amino acid substitutions. Moreover, the gene of the regulatory protein Aro3 was found to contain 23 SNPs, where three caused amino acid substitutions. It is therefore possible that the flux through the shikimate pathway could be different in the two strain backgrounds.

Other features in the two strain backgrounds could influence VG production. For example, in the case of batch cultivation, the higher VG yields in S-VG strains are mainly created after the diauxic shift. This suggests that the S-VG strain has increased activity of the aromatic biosynthetic pathway only at respiratory metabolism, which is consistent with the even higher activity in the glucose limited chemostat cultures. This could be due to a limitation in the supply of erythrose-4-phosphate, a precursor for aromatic amino acid biosynthesis and an intermediate of the pentose-phosphate (PP) pathway. In this context, we note that at fermentative conditions the flux through the PP pathway is much lower than at respiratory conditions (Frick and Wittmann, 2005).

One feature that could influence the final VG yield is availability of co-factors that are required to convert PAC to VG. To this end we note that ATP and UDP-glucose levels seem to be unaffected by the VG pathway in the two strain backgrounds. Moreover, we have previously introduced mutations designed to increase the NADPH/NADP level in the original VG producing strain (S288c background) and this resulted in higher VG levels showing that cofactor availability appears limiting. However, we note that in this study, the organization of the inserted VG pathway genes, including gene copy numbers, in the producer strain is not known (Brochado et al., 2010). We did not measure SAM levels in C-VG and S-VG and this co-factor may vary between the two strains. Similarly, the activity of the PPTase, EntD, which activates ACAR by covalently attaching phosphopantheine to the apoenzyme is unknown and may differ in the two strain backgrounds. Considering the more than 13,000 SNPs between CEN.PK and S288c, one may also expect that differences in the global metabolism may influence VG production. For example, 20 genes in the mitogen-activated protein kinase (MAPK) signaling pathway contain SNPs resulting in amino acid residue substitutions. Among those, one is in Cyr1, which changes the activity through the pathway controlled by the global regulator protein kinase A, PKA (Nijkamp et al., 2012; Vanhalewyn et al., 1999; Tanaka et al., 1990). The ability of the two strains to adapt to toxic intermediates, especially PAL and VAN (Hansen et al., 2009), may also vary and influence yields. Even if they do not, accumulation of these intermediates vary slightly in the two strain back grounds and may therefore differentially influence VG yields. To this end, we note that the growth rates for C-VG and S-VG are reduced as compared to the corresponding strains that do not contain the VG pathway.

Since, the VG yield for S-VG is approximately 20-fold below the maximum theoretical yield; the effects described above are unlikely due to carbon being channeled into the VG pathway at the expense of other destinations and functions. An interesting question that still remains to be answered is therefore how the two strain backgrounds develop as VG producers as yields are improved by e.g. metabolic engineering. Similarly, it would be interesting to address whether some of the obvious genetic differences pointed out above can be transferred from S-VG to C-VG to improve the VG yields in the latter.

5. Concluding remarks

We have shown that heterologous production of VG differs dramatically in two different strain backgrounds. Our analyzes suggest that for strains like CEN.PK and S288c where high quality "-omics" datasets are available it may be possible to predict, which of the two strain backgrounds would be the better producer. As additional data constantly accumulate we expect that such qualified guesses can be made in an increasingly safe manner. However, many other less characterized strain backgrounds exist, and it is likely that one of these strains may be a superior producer of VG. Rapid construction of strains with genetically comparable setups for VG production would be desirable. To this end, we have recently shown that multiple genes can be simultaneously integrated into three different sites in our expression platform in one step by using three different selectable markers (Jensen and Strucko, 2013). Similarly, simultaneous integration of multiple genes have also been achieved via CRISPR-Cas9 technology (Mans et al., 2015; Jakočiūnas et al., 2015) Importantly, since similar strain differences are likely to apply for the production of other metabolites, we strongly recommend to test more than one genetic background during construction of a novel cell factory.

Table 5
Point mutations of *ARO* genes found in CEN.PK113-7D compared to S228c. Mutations represented by one letter code for amino acid and number denoting the position in the protein.

Genes	SNPs		Amino acid substitution
	Total	Non-synonymous	
ARO1	15	7	T225I, P337S, S517P, N844T, M1141K, V1386I, G1576A
ARO3	23	3	K141R, E214D, S349T
ARO4	–	–	–
ARO7	–	–	–

metabolite analyzes; and Anna-Lena Heins and Ted Johansen for facilitating fermentation experiments. This work was supported by Grant 0603-00323B from the Danish Council for Strategic Research.

Appendix A. Supplementary material

Supplementary data associated with this article can be found in the online version at http://dx.doi.org/10.1016/j.meteno.2015.09. 001.

References

Kim, I.-K., Roldão, A., Siewers, V., Nielsen, J., 2012. A systems-level approach for metabolic engineering of yeast cell factories. FEMS Yeast Res. 12 (2), 228–248.

Hong, K.-K., Nielsen, J., 2012. Metabolic engineering of *Saccharomyces cerevisiae*: a key cell factory platform for future biorefineries. Cell. Mol. Life Sci. 69 (16), 2671–2690.

van Dijken, J.P., Bauer, J., Brambilla, L., Duboc, P., Francois, J., Gancedo, C., Giuseppin, M., Heijnen, J., Hoare, M., Lange, H., Madden, E., Niederberger, P., Nielsen, J., Parrou, J., Petit, T., Porro, D., Reuss, M., van Riel, N., Rizzi, M., Steensma, H., Verrips, C., Vindeløv, J., Pronk, J., 2000. An interlaboratory comparison of physiological and genetic properties of four *Saccharomyces cerevisiae* strains. Enzyme Microb. Technol. 26 (9–10), 706–714.

Entian, K., Kötter, P., 2007. Yeast genetic strain and plasmid collections. Methods Microbiol. 36 (06), 629–666.

Goffeau, A., Barrell, B.G., Bussey, H., Davis, R.W., Dujon, B., Feldmann, H., Galibert, F., Hoheisel, J.D., Jacq, C., Johnston, M., Louis, E.J., Mewes, H.W., Murakami, Y., Philippsen, P., Tettelin, H., Oliver, S.G., 1996. Life with 6000 Genes. Sci. 274 , 546–567. http://dx.doi.org/10.1126/science.274.5287.546.

Rogowska-Wrzesinska, A., Larsen, P.M., Blomberg, A., Görg, A., Roepstorff, P., Norbeck, J., Fey, S.J., 2001. Comparison of the proteomes of three yeast wild type strains: CEN.PK2, FY1679 and W303. Comp. Funct. Genom. 2 (4), 207–225.

Canelas, A.B., Harrison, N., Fazio, A., Zhang, J., Pitkänen, J.-P., van den Brink, J., Bakker, B.M., Bogner, E., Bouwman, J., Castrillo, J.I., Cankorur, A., Chumnanpuen, P., Daran-Lapujade, P., Dikicioglu, D., van Eunen, K., Ewald, J.C., Heijnen, J.J., Kirdar, B., Mattila, I., Mensonides, F.I.C., Niebel, A., Penttilä, M., Pronk, J.T., Reuss, M., Salusjärvi, L., Sauer, U., Sherman, D., Siemann-Herzberg, M., Westerhoff, H., de Winde, J., Petranovic, D., Oliver, S.G., Workman, C.T., Zamboni, N., Nielsen, J., 2010. Integrated multilaboratory systems biology reveals differences in protein metabolism between two reference yeast strains. Nat. Commun. 1, 145, http://dx.doi.org/10.1038/ncomms1150.

Daran-Lapujade, P., Daran, J., Kotter, P., Petit, T., Piper, M., Pronk, J., 2003. Comparative genotyping of the laboratory strains S288C and CEN.PK113-7D using oligonucleotide microarrays. FEMS Yeast Res. 4 (3), 259–269.

Otero, J.M., Vongsangnak, W., Asadollahi, M.A., Olivares-Hernandes, R., Maury, J., Farinelli, L., Barlocher, L., Osterås, M., Schalk, M., Clark, A., Nielsen, J., 2010. Whole genome sequencing of *Saccharomyces cerevisiae*: from genotype to phenotype for improved metabolic engineering applications. BMC Genom. 11 (1), 723.

Nijkamp, J.F., van den Broek, M., Datema, E., de Kok, S., Bosman, L., Luttik, M.A., Daran-Lapujade, P., Vongsangnak, W., Nielsen, J., Heijne, W.H.M., Klaassen, P., Paddon, C.J., Platt, D., Kötter, P., van Ham, R.C., Reinders, M.J.T., Pronk, J.T., de Ridder, D., Daran, J.-M., 2012. De novo sequencing, assembly and analysis of the genome of the laboratory strain *Saccharomyces cerevisiae* CEN.PK113-7D, a model for modern industrial biotechnology. Microb. Cell Fact. 11 (1), 36.

Hansen, E.E.H., Møller, B.B.L., Kock, G.R.G., Bünner, C.M., Kristensen, C., Jensen, O.R., Okkels, F.T., Olsen, C.E., Motawia, M.S., Hansen, J., 2009. De novo biosynthesis of vanillin in fission yeast (*Schizosaccharomyces pombe*) and baker's yeast (*Saccharomyces cerevisiae*). Appl. Environ. Microbiol. 75 (9), 2765–2774.

Mikkelsen, M.D., Buron, L.D., Salomonsen, B., Olsen, C.E., Hansen, B.G., Mortensen, U.H., Halkier, B.A., 2012. Microbial production of indolylglucosinolate through engineering of a multi-gene pathway in a versatile yeast expression platform. Metab. Eng. 14 (2), 104–111.

Nørholm, M.H.H., 2010. A mutant Pfu DNA polymerase designed for advanced uracil-excision DNA engineering. BMC Biotechnol. 10, 21.

Geu-Flores, F., Nour-Eldin, H.H., Nielsen, M.T., Halkier, B.A., 2007. USER fusion: a rapid and efficient method for simultaneous fusion and cloning of multiple PCR products. Nucl. Acids Res. 35 (7), e55.

Nour-Eldin, H.H., Hansen, B.G., Nørholm, M.H.H., Jensen, J.K., Halkier, B.A., 2006. Advancing uracil-excision based cloning towards an ideal technique for cloning PCR fragments. Nucl. Acids Res. 34 (18), e122.

Mortimer, R.K., Johnston, J.R., 1986. Genealogy of principal strains of the yeast genetic stock center. Genetics 113 (1), 35–43.

Gietz, D., Jean, A. St., Woods, R.A., Schiestl, R.H., 1992. Improved method for high efficiency transformation of intact yeast cells. Nucl. Acids Res. 20 (6), 1425.

Boeke, J.D., Lacroute, F., Fink, G.R., 1984. Short communication: a positive selection for mutants lacking orotidine-5′-phosphate decarboxylase activity in yeast : 5-fluoro-orotic acid resistance. Mol. Gen. Genet., 345–346.

Güldener, U., Heck, S., Fielder, T., Beinhauer, J., Hegemann, J.H., 1996. A new efficient gene disruption cassette for repeated use in budding yeast. Nucl. Acids Res. 24 (13), 2519–2524.

Treco, D.A., Winston, F., 2008. Growth and manipulation of yeast. Curr. Protoc. Mol. Biol. 13 (vol. Chapter 13, no. April, p. Unit).

Bertani, G., 1951. Studies on lysogenesis. I. The mode of phage liberation by lysogenic *Escherichia coli*. J. Bacteriol. 62 (3), 293–300.

Sherman, F., Fink, G.R., Hicks, J.B., 1986. Laboratory Course Manual for Methods in Yeast Genetics. Cold Spring Harbor Laboratory.

Verduyn, C., Postma, E., Scheffers, W.A., Van Dijken, J.P., 1992. Effect of benzoic acid on metabolic fluxes in yeasts: a continuous-culture study on the regulation of respiration and alcoholic fermentation. Yeast 8 (7), 501–517.

Olsson, L., Nielsen, J., 1997. On-line and in situ monitoring of biomass in submerged cultivations. Trends Biotechnol. 15, 517–522.

Villas-Bôas, S.G., Højer-Pedersen, J., Akesson, M., Smedsgaard, J., Nielsen, J., 2005. Global metabolite analysis of yeast: evaluation of sample preparation methods. Yeast 22 (14), 1155–1169.

Magdenoska, O., Martinussen, J., Thykaer, J., Nielsen, K.F., 2013. Dispersive solid phase extraction combined with ion-pair ultra high-performance liquid chromatography tandem mass spectrometry for quantification of nucleotides in *Lactococcus lactis*. Anal. Biochem. 440 (2), 166–177.

Van Hoek, P., 1998. Effect of specific growth rate on fermentative capacity of baker's yeast. Appl. Environ. 64 (11), 4226–4233.

Brochado, A.R., Matos, C., Møller, B.L., Hansen, J., Mortensen, U.H., Patil, K.R., 2010. Improved vanillin production in baker's yeast through in silico design. Microb. Cell Fact. 9 (1), 84.

Nevoigt, E., 2008. Progress in metabolic engineering of *Saccharomyces cerevisiae*. Microbiol. Mol. Biol. Rev. 72 (3), 379–412.

Teshiba, S., Furter, R., Niederberger, P., Braus, G., Paravicini, G., Hütter, R., 1986. Cloning of the ARO3 gene of *Saccharomyces cerevisiae* and its regulation. Mol. Gen. Genet. 205 (2), 353–357.

Braus, G.H., 1991. Aromatic amino acid biosynthesis in the yeast *Saccharomyces cerevisiae*: a model system for the regulation of a eukaryotic biosynthetic pathway. Microbiol. Rev. 55 (3), 349–370.

Luttik, M.A.H., Vuralhan, Z., Suir, E., Braus, G.H., Pronk, J.T., Daran, J.M., 2008. Alleviation of feedback inhibition in *Saccharomyces cerevisiae* aromatic amino acid biosynthesis: quantification of metabolic impact. Metab. Eng. 10 (3–4), 141–153.

Koopman, F., Beekwilder, J., Crimi, B., van Houwelingen, A., Hall, R.D., Bosch, D., van Maris, A.J.A., Pronk, J.T., Daran, J.-M., 2012. De novo production of the flavonoid naringenin in engineered *Saccharomyces cerevisiae*. Microb. Cell Fact. 11, 155.

Hong, K.-K., Hou, J., Shoaie, S., Nielsen, J., Bordel, S., 2012. Dynamic 13C-labeling experiments prove important differences in protein turnover rate between two *Saccharomyces cerevisiae* strains. FEMS Yeast Res. 12 (7), 741–747.

Frick, O., Wittmann, C., 2005. Characterization of the metabolic shift between oxidative and fermentative growth in *Saccharomyces cerevisiae* by comparative ^{13}C flux analysis. Microb. Cell Fact. 4, 30.

Vanhalewyn, M., Dumortier, F., Debast, G., Colombo, S., Ma, P., Winderickx, J., Van Dijck, P., Thevelein, J.M., 1999. A mutation in Saccharomyces cerevisiae adenylate cyclase, $Cyr1^{K1876M}$, specifically affects glucose- and acidification-induced cAMP signalling and not the basal cAMP level. Mol. Microbiol. 33, 363–376. http://dx.doi.org/10.1046/j.1365-2958.1999.01479.x.

Tanaka, K., Nakafuku, M., Satoh, T., Marshall, M.S., Gibbs, J.B., Matsumoto, K., Kaziro, Y., Toh-e, A., 1990. *S. cerevisiae* genes IRA1 and IRA2 encode proteins that may be functionally equivalent to mammalian ras GTPase activating protein. Cell 60 (5), 803–807.

Jensen, N.B., Strucko, T., Kildegaard, K.R., David, F., Maury, J., Mortensen, U.H., Forster, J., Nielsen, J., Borodina, I., 2014. EasyClone: method for iterative chromosomal integration of multiple genes in Saccharomyces cerevisiae. FEMS Yeast Res. 14, 238–248. http://dx.doi.org/10.1111/1567-1364.12118.

Mans, R., van Rossum, H.M., Wijsman, M., Backx, A., Kuijpers, N.G.A., van den Broek, M., Daran-Lapujade, P., Pronk, J.T., van Maris, A.J.A., Daran, J.-M.G., 2015. CRISPR/Cas9: a molecular Swiss army knife for simultaneous introduction of multiple genetic modifications in *Saccharomyces cerevisiae*. FEMS Yeast Res., 1–15.

Jakočiūnas, T., Bonde, I., Herrgård, M., Harrison, S.J., Kristensen, M., Pedersen, L.E., Jensen, M.K., Keasling, J.D., 2015. Multiplex metabolic pathway engineering using CRISPR/Cas9 in *Saccharomyces cerevisiae*. Metab. Eng. 28, 213–222.

Partow, S., Siewers, V., Bjørn, S., Nielsen, J., Maury, J., 2010. Characterization of different promoters for designing a new expression vector in Saccharomyces cerevisiae. Yeast 27, 955–964. http://dx.doi.org/10.1002/yea.1806.

Nakagawa, S., Niimura, Y., Gojobori, T., Tanaka, H., Miura, K., 2008. Diversity of preferred nucleotide sequences around the translation initiation codon in eukaryote genomes. Nucl. Acids Res. 36 (3), 861–871.

Cavener, D.R., Ray, S.C., 1991. Eukaryotic start and stop translation sites. Nucl. Acids Res. 19 (12), 3185–3192.

Lange, H.C., Heijnen, J.J., 2001. Statistical reconciliation of the elemental and molecular biomass composition of *Saccharomyces cerevisiae*. Biotechnol. Bioeng. 75 (3), 334–344.